Calibration of DEM Parameters for Multi-Component Segregation

Hadi, A.H.; Pang, Y.; Schott, D.L.

Publication date
2023

Document Version
Final published version

Citation (APA)
Hadi, A. H., Pang, Y., & Schott, D. L. (2023). *Calibration of DEM Parameters for Multi-Component Segregation*. Paper presented at ICBMH 2023: 14th International Conference on Bulk Materials Storage, Handling and Transportation, Wollongong, Australia.

ICBMH2023 - The 14th International Conference on Bulk Materials Storage, Handling and Transportation
11-13th July, 2023, Wollongong, New South Wales, Australia

Calibration of DEM Parameters for Multi-Component Segregation

Ahmed Hadi, Yusong Pang and Dingena L. Schott

Department of Maritime and Transport Technology, Faculty of Mechanical, Maritime and Materials Engineering, Delft University of Technology, Delft, 2628CD, The Netherlands

ABSTRACT Segregation or de-mixing is the phenomenon occurring in moving granular materials in which particles with similar properties, e.g., size, density and shape, accumulate. This de-mixing reduces the homogeneity of the mixture which is generally considered undesirable and should be minimised. Despite many experimental and numerical attempts to investigate segregation in relation to different factors, the current literature has several shortcomings. Firstly, most of these studies have considered single-component mixtures, usually with a limited number of particle diameters, while most of the mixtures existing in industry and nature are complex multi-component mixtures. Secondly, a systematic calibration procedure for segregation is often missing while it is crucial for developing a reliable and predictive DEM model.

This study proposes a combined global and local calibration strategy for DEM modelling of multi-component segregation. We demonstrate this for an iron ore mixture (i.e., the mixture of pellets and sinter), which is a good example of a multi-component mixture. The model was calibrated not only on the global level but also on the local level and hence it consists of two steps. First, pellets and sinter were individually calibrated on bulk level using the angle of repose measured in a shear box setup. Second, mixtures of pellets and sinter were discharged into a transparent quasi-3D hopper and the segregation index was used to calibrate the interaction parameters between pellets and sinter on a local level. Hereby, image analysis in conjunction with painting pellets have been utilised to measure segregation in a non-invasive manner. We conclude that the initial results of the proposed calibration procedure are promising. To improve it further, we suggest utilizing a more manageable experimental setup, improving the simulation model for the mixture, reducing the number of potential parameter sets, and testing other parameters resulting from single-component calibration.

1. INTRODUCTION

Granular segregation is a well-known phenomenon in which particles with similar properties, such as size, density and shape, tend to accumulate in specific spatial locations of the bulk materials. It occurs only when bulk materials are in motion under external forces like gravity. In most industrial applications, segregation is considered an undesirable occurrence since it can affect product homogeneity adversely. Reducing or controlling segregation can improve the efficiency of the relevant industrial processes, resulting in lower energy consumption, less waste due to better material utilisation and lower greenhouse gas emissions, all paving the way for a more sustainable future. Granular segregation has been investigated experimentally since the early 70s [1–3]. However, experimental investigation of segregation is limited due to difficulties in accurately measuring granular composition, the inability to gather comprehensive particle-scale data and the high cost and time required for studying various factors that affect segregation.

The Discrete Element Method (DEM), initially introduced by Cundall and Strack [4], has become a widely used tool for modelling granular phenomena. DEM can provide particle-level insight into segregation patterns that are difficult and expensive to achieve experimentally, making it a practical tool for modelling and optimizing industrial processes dealing with segregation. However, besides being computationally expensive, the main challenge is to calibrate the DEM model in order to make it a trustable tool which represents the real-world behaviour of granular materials. Despite the great number of past studies on DEM modelling of segregation, only a few attempted to calibrate the model [5–7]. Furthermore, most of the past studies focussed on modelling segregation in binary- or ternary-sized mixture. However, most of the mixtures in industrial applications are composed of two or more components, each having a size distribution.

This study aims at developing a systematic DEM calibration procedure for the segregation of multi-component mixtures. We demonstrate this for a mixture of pellets and sinter, which is an example of a multi-component mixture in the blast furnace charging system. First, we provide an explanation of the experimental measurements that are necessary for determining material properties or calibrating the model. Then, we introduce our approach to calibration, accompanied by the simulation results.

2. EXPERIMENTS

This section covers experimental measurements that can be divided into three categories: 1) material properties, 2) bulk calibration experiments, and 3) segregation tests. Each category is described in detail in the following paragraphs. In this research, image analysis is used to measure segregation non-intrusively. However, sinter and pellets have similar colours, making it difficult to segment the image. To solve this issue, we painted pellets with a distinguishing white colour. To ensure that painting the pellets did not affect their frictional characteristics, we conducted a comparison of the angle of repose in the ledge test between painted and unpainted pellets. The results showed that there were no significant differences between the two groups (i.e. 40.4° ± 2.1° for unpainted pellets and 40.5° ± 1.1° for painted ones), indicating that painting the pellets did not affect their frictional properties.

2.1. Material Properties

We directly measured particle size distribution, particle density and particle-geometry coefficient of sliding friction. First, the particle size distribution (PSD) of pellets and sinter were measured through manual sieving, which is shown in Figure 1. Next, we measured particle density using a pycnometer, resulting in 4322 kg/m^3 and 4632 kg/m^3 for sinter and pellets, respectively.

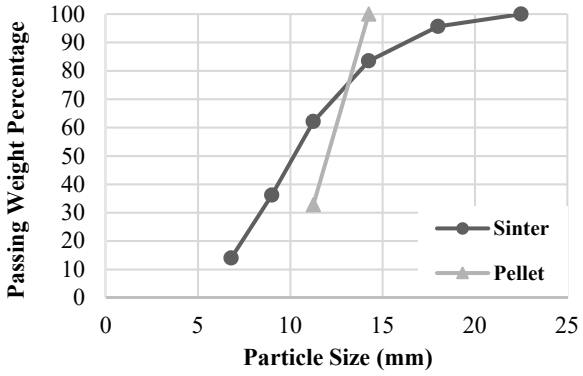

Figure 1 Measured Size Distribution of Pellets and Sinter

In the next step, we used an inclined surface tester as shown in Figure 2a to measure the particle-geometry coefficient of sliding friction [8,9]. The test starts with the surface being horizontal, after which particles are placed on it. The surface then begins to rotate gradually until the particles start sliding. Having the angle at which particles begin to slide (θ_w), the coefficient of sliding friction between particles and the surface can be calculated using the following equation:

$$\mu_{s_{p-g}} = \tan\theta_w \tag{1}$$

Unlike sinter particles, pellets are nearly spherical and have a tendency to roll before sliding. To restrain the rolling behaviour, we glued four pellet particles together and then placed them on the surface (cf. Figure 2b). Moreover, because sinter particles have a comparably wide size distribution, we selected 6 particles with different sizes to measure the coefficient of sliding friction. We repeated the measurements ten times for the glued pellets and five times for each sinter particle. The 95% confidence intervals of the measured particle-wall sliding friction coefficients were 0.36 ± 0.015 and 0.4 ± 0.02 for pellets and sinter, respectively.

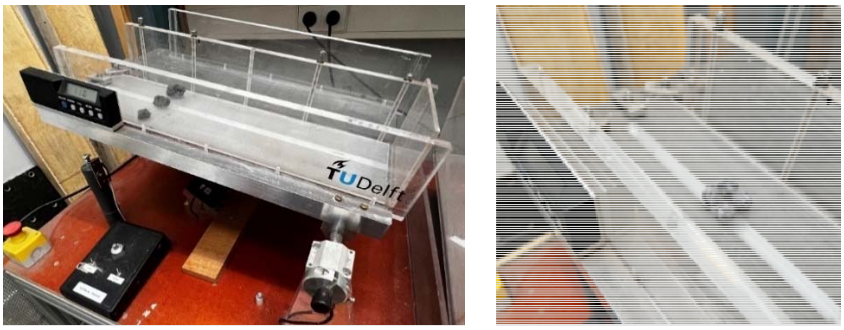

(a) (b)

Figure 2 a) Inclined Surface Test Setup, b) Four Pellets Glued Together

2.2. Bulk Calibration Experiments

Bulk experiments include measuring the angle of repose in the ledge test and filling the bin test. The ledge test box is shown in Figure 3a. The size of the box is 200×140×200 mm (L×W×H). Conducting the angle of repose test in the ledge box simply involves pouring materials into the box with a closed door (cf. Figure 3b). Then, the door is opened and materials begin discharging out of the box until a steady slope is formed inside the box, whose slope represents the angle of repose (cf. Figure 3c).

(a) (b) (c)

Figure 3 a) Ledge Test Box, b) Filled Ledge Box, and c) the Slope Formed at the End of the Test

In this work, we measure the angle using image analysis as follows. First, we cropped the image to focus on the region of interest (ROI), as shown in Figure 4a, which we define as the portion of the slope that is sufficiently distant from the side walls. Next, we replace the original background of the cropped image with an ideally green colour to facilitate image analysis in the next step (cf. Figure 4b). Then, we employed image processing to segment the image and extract the edge of the slope, as in Figure 4c. After that, a linear line is fitted on the edge, whose slope represents the angle of repose.

The experimental setup of the second experiment, i.e. filling the bin test, is shown in Figure 5a, and the dimensions can be seen in Figure 5b. We charged materials at the top into the bin using a bucket, which is a cylinder with a diameter of 300 mm and a height of 290 mm. Then, we took a photo of the heap formed in the bin and applied the same procedure as for the ledge test to measure the angle of repose.

A summary of the results of the angle of repose measurements for pellets and sinter in the ledge test as well as the filling the bin test are presented in Table 1.

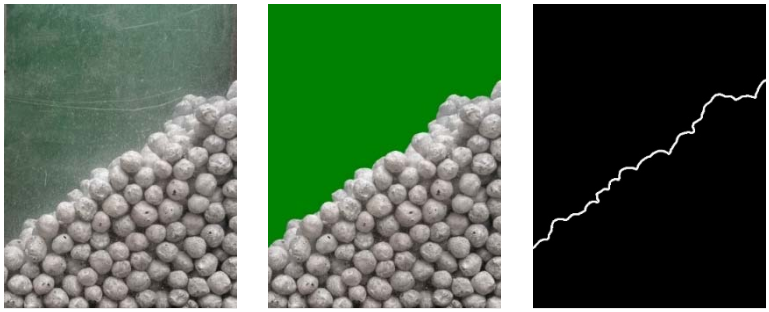

(a) (b) (c)

Figure 4 a) Cropped Region of Interest, b) Post-Processed Image, and c) Extracted Edge of the Slope

(a) (b)

Figure 5 Filling the Bin Test a) Experimental Setup, and b) Schematic View and Dimensions

Table 1 Experimental Results of AoR (95% CI, n = 5 (Ledge Test) and 3 (Bin Test))

	Ledge Test	Filling the Bin Test
Pellet	40.5° ± 1.1°	26.7° ± 1.3°
Sinter	45.9° ± 1.8°	21.7° ± 0.7°

2.3. Segregation Tests

As the focus of this paper is to develop a DEM model for segregation, it is essential to measure segregation as a local occurrence, rather than relying only on the global behaviour such as the angle of repose. The results of segregation measurements can be used as a key performance indicator (KPI) to calibrate the model. To do this, we conduct the "filling the bin" test similar to the one mentioned above. However, here, we charged pellets and sinter together into the bin. To make the initial mixture configuration reproducible, we put the pellets and sinter in three separate layers into the bucket as schematically illustrated in Figure 6. Then, we charged pellets and sinter into the bin to form a heap, as shown in

Figure 7a (left), and we repeated the experiments four times. Then we took images from the heap then we post processed them as explained above for single-component experiments. We measured two KPIs in the heap using image analysis: KPI1, the angle of repose similar to that of single-component calibration (cf.

Figure 7a (right)), and KPI2, the Relative Standard Deviation (RSD) as a segregation index [7,10]. In order to calculate this index, we segmented the image into two different figures, as in

Figure 7b (left) and (right), in which white pixels represent pellets and sinter particles, respectively. Then, we applied a grid system to split the segmented figure into a number of sub-figures, which we call "tiles". The size of tiles is 100 mm, nearly 4-5 times the largest particle size. In each tile, we extracted the area of white pixels for pellets and sinter in pixels. Having these areas in each tile, the pixel fraction for the component i in the kth tile is calculated as follows:

$$C_{i_k} = \frac{N_{i_k}}{\sum_{i=1}^{n} N_{i_k}} \tag{2}$$

Where N_{i_k} is the pixel number of component i in the kth tile and n denotes the total number of components (here two, i.e. pellets and sinter). To reduce errors, we excluded tiles that are occupied less than 20 percent from the calculation. Then, the average (μ_i) and standard deviation (σ_i) of C_{i_k} are calculated over all tiles for each component and RSD is given as:

$$RSD_i = \frac{\sigma_i}{\mu_i} \tag{3}$$

The results of the experimental measurements for KPI1 and KPI2 are presented in Table 2.

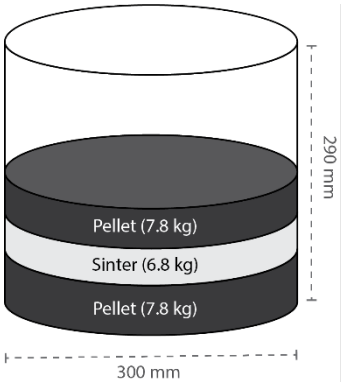

Figure 6 The Layered Configuration of Pellets and Sinter Used in the Bucket for the Segregation Test

3. DISCRETE ELEMENT METHOD (DEM)

Using Newton's second law through numerical integration, a DEM model determines the positions of particles at each time step by computing the forces and moments of inertia acting on them. The interaction forces are determined by a contact model. In this paper, we use Hertz-Mindlin (no slip) contact model [11] with rolling friction type C [12,13]. This rolling friction model has been shown to yield good results while reducing the number of parameters to be calibrated [14]. Regarding the particle shape, as pellets are nearly spheres, the spherical shape is suitable to model them. However, sinter particles are highly irregular in shape and this needs to be accurately modelled for segregation [6]. A clumped sphere approach can be adopted to model their irregular shape. Considering the fact that increasing the number of spheres in the clumped approach significantly increases the computational time, we use a three-sphere clumped particle (cf. Figure 8), which has been shown to deliver good results in previous studies on sinter [15,16]. We utilised EDEM version 2022.2 to carry out DEM simulations.

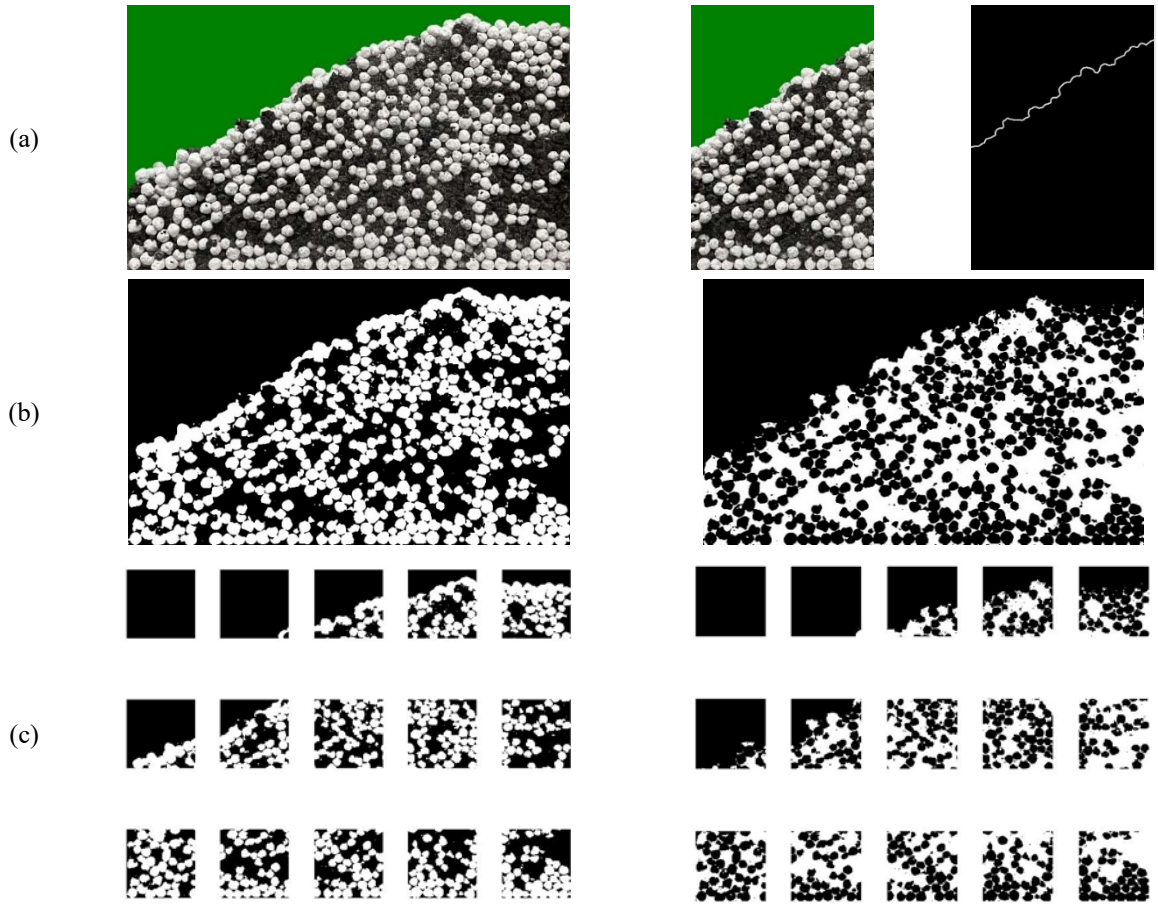

Figure 7 a) Post-Processed Photo of the Heap (Left), Cropped Region of Interest (Middle) and Extracted Edge of the Heap (Right), b) Segmented Images, and c) Split Images into Tiles

Table 2 Experimental Results of the Segregation Test (95% CI, n=3)

	KPI1 (AoR)	KPI2	
		RSD (Pellet)	RSD (Sinter)
Results	30.34° ± 2.71°	0.165 ± 0.023	0.164 ± 0.04

Figure 8 The Clumped-Sphere Shape Used to Model Sinter Particles

3.1. Calibration Procedure

Taking the Hertz-Mindlin contact model with rolling friction type C into account, all the parameters necessary to define a DEM model for the mixture of pellet and sinter as well as the approach for determining them are listed in Table 3. In Table 3, bulk calibration refers to the calibration of parameters by replicating the bulk behaviour at the global level (i.e. experiments mentioned in section 2.2). However, in local calibration, attempts are made to mimic the local behaviour, i.e. segregation-related measurements, of granular materials as mentioned in section 2.3. An

overview of the calibration procedure is illustrated in Figure 9, which is mainly based on the calibration order proposed by Katterfeld et al. [17].

Table 3 An Overview of DEM Parameters and the Approach for Determining Them

Category	DEM Parameter	Sinter	Pellet	Sinter-Pellet
Intrinsic Particle Properties	Shear modulus (G)	Literature	Literature	N/A
	Poisson's ratio (υ)	Literature	Literature	N/A
	Size distribution	Direct measurement	Direct measurement	N/A
	Particle density (ρ_s)	Direct measurement & bulk calibration	Direct measurement & bulk calibration	N/A
	Particle shape	Clumped spheres (from literature)	Sphere	N/A
Particle-Particle Interaction	Coefficient of sliding friction ($\mu_{s,pp}$)	Bulk calibration	Bulk calibration	Bulk calibration & local calibration
	Coefficient of rolling friction ($\mu_{r,pp}$)	Bulk calibration	Bulk calibration	Bulk calibration & local calibration
	Coefficient of restitution ($C_{r,pp}$)	Literature	Literature	Average
Particle-Geometry Interaction	Coefficient of sliding friction ($\mu_{s,pw}$)	Direct measurement	Direct measurement	N/A
	Coefficient of rolling friction ($\mu_{r,pw}$)	Literature	Literature	N/A
	Coefficient of restitution ($C_{r,pw}$)	Literature	Literature	N/A

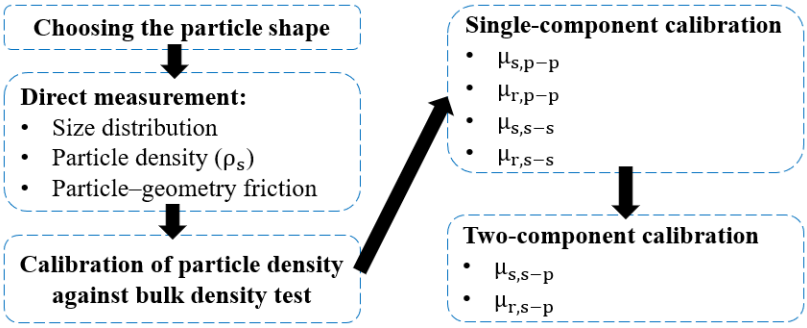

Figure 9 An Overview of the Calibration Strategy Used in this Study

According to Coetzee [18], particle density needs to be calibrated against the bulk density measurement to account for the simplifications in the modelling of particle size and shape. To accomplish this, we measured bulk density by filling a cylindrical container with a known volume. Then, we modelled the same container and filled it with particles in DEM simulations. Since bulk density is mainly dependent on particle density, we took all the other parameters at this stage from relevant literature [16,19–21]. We then adjusted the particle density in DEM iteratively until the modelled bulk density matched the measured one, where we obtained the calibrated particle density as 3500 kg/m^3 and 3985 kg/m^3 for sinter and pellets, respectively. Table 4 presents a summary of all the base parameters that have been already measured, calibrated, or sourced from literature, with the exception of the coefficients of sliding and rolling friction for particle-particle interactions, which will be calibrated in this work.

The calibration process focuses on finding the suitable values for the coefficients of sliding and rolling friction between pellets, sinter and their interaction. We have selected these parameters as targets for calibration because according to Wensrich et al. [22], the macroscopic behaviour of free-flowing bulk materials is mainly influenced by coefficients of friction. The proposed calibration approach contains two steps: step 1 where we calibrate each component (i.e. sinter or pellets) individually, and step 2, where we calibrate the interaction parameters between pellets and sinter by comparing the simulation results with experiments on the mixture. These two steps and the simulation results are explained in the following paragraphs.

Table 4 Base DEM Parameter Values Used in this Study

DEM Parameter	Source	Pellet	Sinter
Bulk density (kg/m^3)	Measured	1951 ± 7	1731 ± 7
Particle density (kg/m^3)	Measured	4632	4322
	Calibrated	3985	3500
Shear modulus (Pa)		1e+8 [16]	1e+8 [16]
Poisson's ratio		0.25 [16]	0.25 [16]
Particle-geometry sliding friction	Measured	0.36	0.4
Particle-geometry rolling friction		0.16 [19]	0.08 [16]
Coefficient of restitution	Particle-particle	0.42 [19]	0.35 [19]
	Particle-geometry	0.4 [19]	0.4 [19]

3.1.1 Single-Component Calibration

In this step, the coefficients of sliding and rolling friction for pellet-pellet and sinter-sinter are calibrated. Because for each component two parameters need to be calibrated, we use the angle of repose measured in the ledge test and in the bin (cf. section 2.2) as KPIs. Although both KPIs are of the same nature, the flow regime can be assumed different as in the ledge test it is more static compared to filling the bin from the top, where a quasi-dynamic regime is expected. Hence, it would be expected that KPI2 limits the number of permissible combinations of the coefficients of sliding and rolling friction. At this stage, we used the material properties mentioned in Table 4. Then, we varied the coefficients of sliding and rolling friction for pellet-pellet and sinter-sinter. To reduce the number of simulations, we have limited the range of these parameters based on the existing literature [21] (see **Error! Reference source not found.**). To be consistent, we measured the angle of repose in the ledge test model with exactly the same approach as in experiments, i.e. using image analysis. Results of DEM simulations of ledge test for pellets and sinter are shown in Figure 10a and Figure 10b. The grey-coloured area represents the reference based on the experimental results. This means that all the possible combinations of the coefficients of sliding and rolling friction which fall in this area can yield the same angle of repose as the one measured in the experiments. Next, as illustrated in Figure 10c, we superimposed the contour plots of the ledge test and filling the bin tests for pellets and sinter to find the area which satisfies both KPIs. As can be seen, there are still infinite possibilities for the combination of the parameters that satisfy the experimental results. Since the pellet-pellet and sinter-sinter coefficients of sliding and rolling friction are needed for the next calibration step, we picked three pairs of them for pellets (i.e., P1, P2 and P3 in Figure 10c (left)) as well as three for sinter (i.e. S1, S2 and S3 in Figure 10c (right)). We selected these three pairs in such a way that we include low sliding/ high rolling (i.e. P1 and S1), medium sliding/ medium rolling (i.e. P2 and S2) and high sliding/ low rolling (i.e. P3 and S3) combinations of the friction coefficients, as shown in Figure 10c.

Table 5 The Range of the Parameters Used in the Calibration of Pellets and Sinter

	Coefficient of Sliding Friction	Coefficient of Rolling Friction
Pellet	0.3:0.1:0.9	0.2:0.05:0.5
Sinter	0.2:0.1:0.7	0.0:0.05:0.25

3.1.2 Two-Component Calibration

After calibrating each component separately, the interaction parameters between pellets and sinter (i.e. pellet-sinter coefficients of sliding and rolling friction) are calibrated in this step. Similar to single-component calibration, a minimum of two KPIs are required to limit the number of permissible combinations of two parameters. These two KPIs are measured in a single experiment (i.e. segregation experiment) as explained below.

Considering the three pairs of coefficients of sliding and rolling friction for pellets and sinter mentioned in Figure 10c, a total of nine combinations is possible. We name these combinations P1S1, P1S2, …, P3S3. Initially, we employed KPI1, which is the angle of repose for the mixture, to screen out the nine combinations and determine the best potential solution. At this stage, we assumed the coefficients of sliding and rolling friction for sinter-pellet contact to be the average of those for sinter-sinter and pellet-pellet contacts. The simulation was conducted five

times for each combination, and the outcomes (95% confidence interval) are presented in Figure 11. As can be seen, the interaction parameters have an influence on the angle of repose of the mixture. Here we conclude P3S3 combination yields the best match between simulations and the experimental angle of repose. Hence, we continue to calibrate the DEM model against KPI2 with the P3S3 combination.

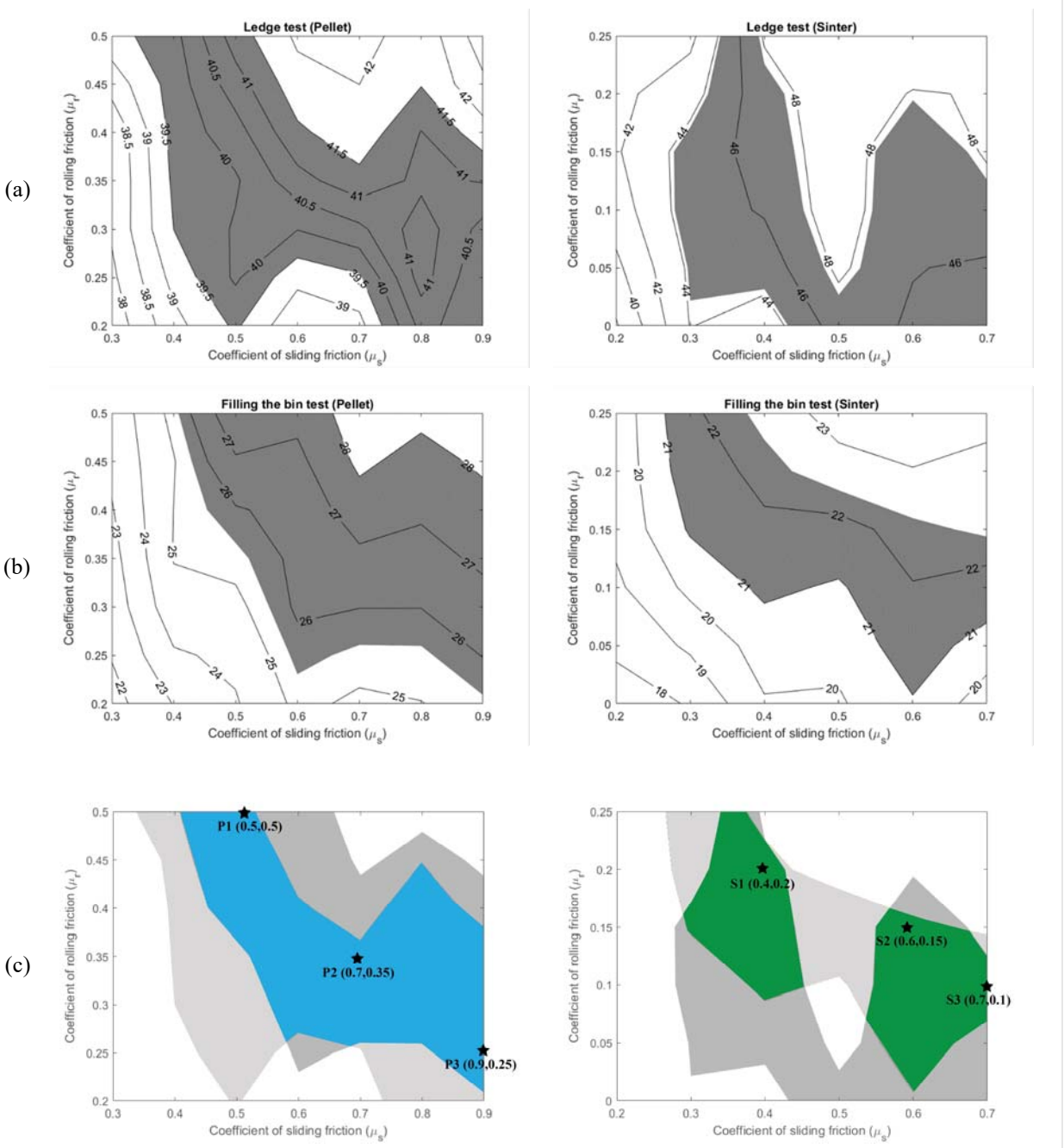

Figure 10 Results of the DEM Simulations, a) Ledge Test for Pellets (Left) and Sinter (Right), b) Filling the Bin Test for Pellets (Left) and Sinter (Right), and c) Superimpositions of Permissible Combinations of Both Tests for Pellets (Left) and Sinter (Right)

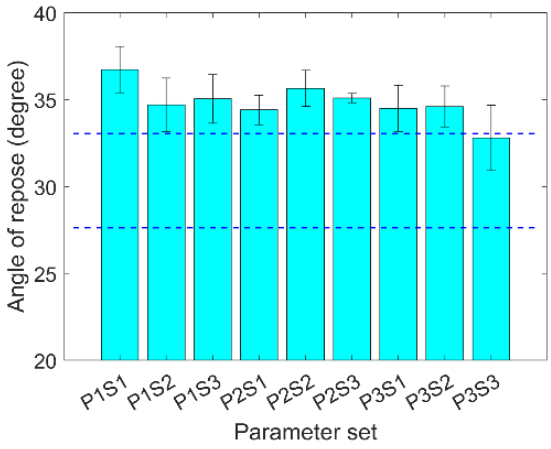

Figure 11 Results of AoR in DEM Simulations of Nine Parameter Combinations (Dashed Lines Represent the Lower and Upper Bounds of the 95% CI of the Experiments)

Next, we varied the pellet-sinter coefficients of sliding and rolling friction as presented in Table 6, in which we assumed that the coefficients of sliding and rolling friction for pellet-sinter contacts fall between those of pellet-pellet and sinter-sinter contacts. Each simulation was carried out five times to ensure statistical rigour. To maintain consistency in our approach to measuring segregation, we captured screenshots of DEM simulations and employed image analysis to quantify segregation, similar to the aforementioned method utilized in the experiments. The results in terms of RSD for pellets and sinter are presented in Figure 12, in which blue dashed lines represent the lower and upper bounds of experimental measurements of the 95% confidence interval. While all the combinations for pellet-sinter coefficients of sliding and rolling frictions give adequate RSD values of sinter particles, only a selection of them, i.e. 1,2,4,5,7,9,10 and 12, yield satisfactory results for the RSD of pellets. From these sets, 1, 2, 4, 5 and 7 give a reasonable estimate in the range of the experimentally measured AoR (Figure 13). Therefore, these parameter sets (the underlined sets in Table 6) can be considered as calibrated pellet-sinter interaction coefficients.

4. DISCUSSION

Figure 14 presents an example of experimental and simulated results, showing a qualitatively good agreement on segregation. However, as could be observed from Figure 11 and Figure 12, the AoR results of the simulations are on the high side and deviate to some extent from the experimental results and are not yet adequately conclusive. Such deviation can be attributed to the inability to reproduce the experimental setup with the mixture precisely (e.g. the bucket position and rotating speed). In the simulation setup, material accumulates at the top entrance of the bin which reduced the material velocity and consequently might have led to a higher angle of repose. Other causes could include the possible omission of more "promising" parameter sets from the enormous array shown in Figure 10c, and, the exclusion of other parameters from calibration such as the coefficient of restitution could significantly impact the results. The next steps to enhance our proposed combined global and local calibration strategy for multi-component mixtures include utilizing a more controllable experimental setup, enhancing the simulation model for the mixture, reducing the number of potential parameter sets, and testing other parameters resulting from single-component calibration.

Table 6 Simulation Matrix Used for the Coefficient of Sliding and Rolling Frictions for Pellet-Sinter Interaction. The Parameter Sets are Indicated by 1..12, and the Calibrated Combinations are Underlined

		Coef. of Sliding Friction		
		0.7	**0.8**	**0.9**
Coef. of Rolling Friction	**0.1**	1	2	3
	0.15	4	5	6
	0.2	7	8	9
	0.25	10	11	12

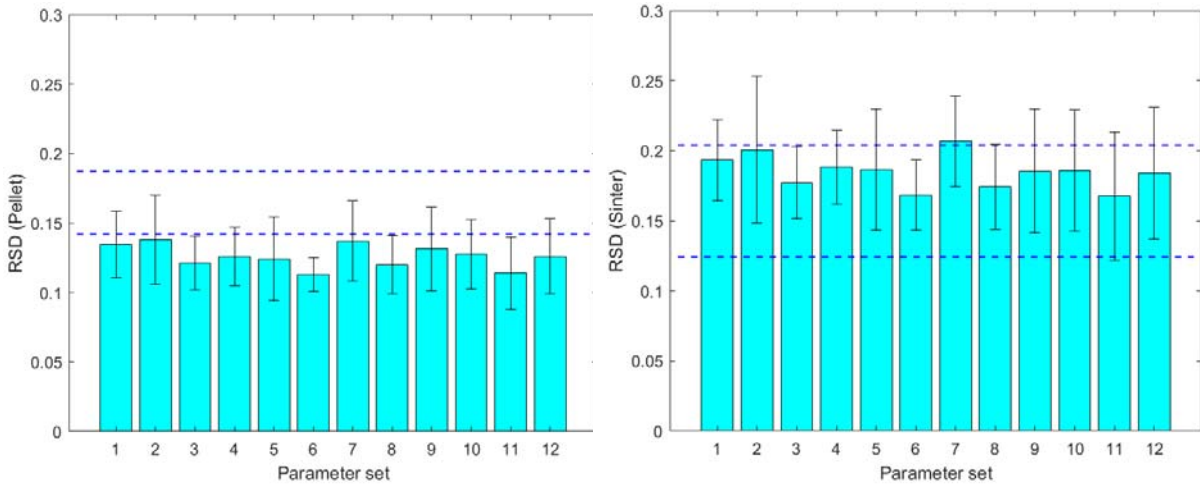

(a) (b)

Figure 12 Segregation Results of DEM Simulations for Twelve Combinations as Listed in Table 6, a) RSD of Pellets, and b) RSD of Sinter Table 6

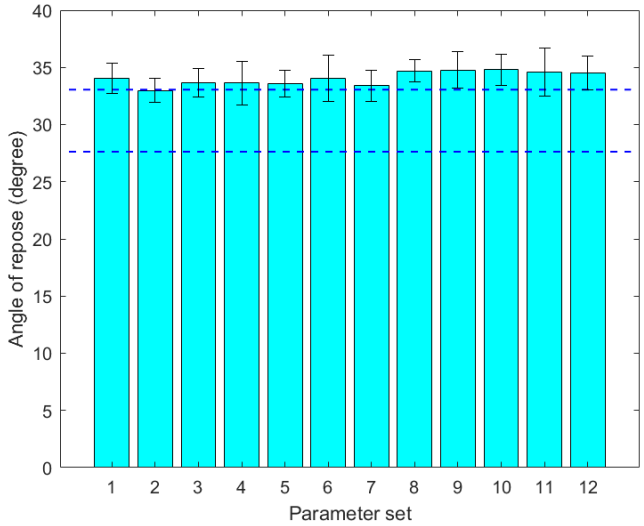

Figure 13 Results of AoR of the Mixture in Twelve Possible Combinations as Listed in Table 6

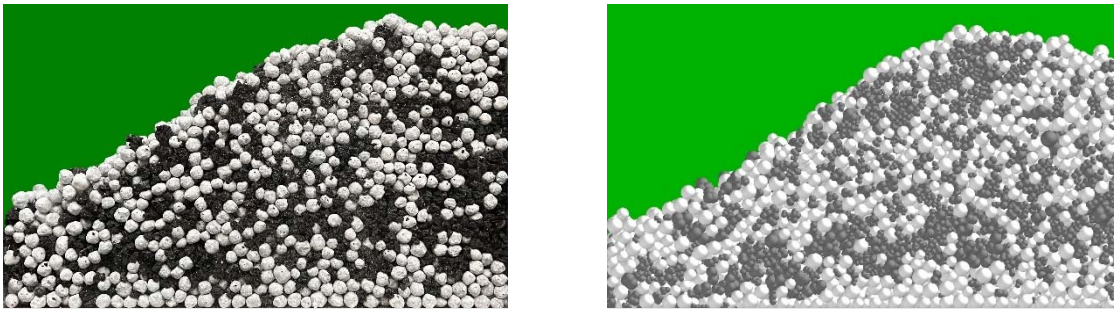

(a) (b)

Figure 14 Results of Multi-Component Mixture of Sinter (Black) and Pellets (White) a) Experiments and b) Calibrated DEM Model Output Based on Parameter Set 2 (see Table 6).

5. CONCLUSION

This study proposes a combined global and local calibration strategy for DEM modelling of multi-component segregation. The two-step calibration strategy first calibrates both single components (pellets and sinter) separately against global behaviour (angle of repose), and second, calibrates the sinter-pellet interaction parameters against local behaviour (segregation-related measurements). The main findings of the present study are as follows:

- The proposed calibration approach is overall promising. The initial results demonstrate an adequately calibrated material for the segregation of one of the components, with a slight overestimation of the global characteristics (angle of repose). Improved results are expected by modifying the setup and employing a more controlled one.
- All permissible combinations of sliding and rolling friction could reproduce the RSD of sinter particles, however, the segregation behaviour of pellets was generally underestimated. Therefore, to calibrate a DEM model for multi-component segregation, segregation measurements of all components are necessary.
- The sliding and rolling friction for pellet-sinter interaction does not appear to significantly influence the angle of repose as well as the segregation results. This could be attributed to the low sensitivity of segregation to these parameters. Therefore, it is recommended to incorporate a broader parameter sensitivity analysis into future DEM calibration studies on segregation.

Future work includes utilizing a more controllable experimental setup, enhancing the simulation model for the mixture, reducing the number of potential parameter sets, and testing other parameters resulting from single-component calibration.

6. ACKNOWLEDGEMENTS

This research was carried out under project number T18019 in the framework of the Research Program of the Materials innovation institute (M2i) (www.m2i.nl) supported by the Dutch government.

7. REFERENCES

[1] K. Shlnohara, S.I. Mlyata, Mechanism of Density Segregation of Particles in Filling Vessels, Ind. Eng. Chem. Process Des. Dev. 23 (1984) 423–428. https://doi.org/10.1021/i200026a003.
[2] S.P. Duffy, V.M. Puri, Primary segregation shear cell for size-segregation analysis of binary mixtures, KONA Powder Part. J. 20 (2002) 196–207. https://doi.org/10.14356/kona.2002022.
[3] J. Williams, Mixing and Segregation in Powders, in: Princ. Powder Technol., 1990: pp. 71–90.
[4] P.A. Cundall, O.D.L. Strack, A discrete numerical model for granular assemblies, Geotechnique. 29 (1979) 47–65. https://doi.org/10.1680/geot.1979.29.1.47.
[5] M. Combarros, H.J. Feise, H. Zetzener, A. Kwade, Segregation of particulate solids: Experiments and DEM simulations, Particuology. 12 (2014) 25–32. https://doi.org/10.1016/j.partic.2013.04.005.
[6] M. Combarros Garcia, H.J. Feise, S. Strege, A. Kwade, Segregation in heaps and silos: Comparison between experiment, simulation and continuum model, Powder Technol. 293 (2016) 26–36. https://doi.org/10.1016/j.powtec.2015.09.036.
[7] M. Alizadeh, A. Hassanpour, M. Pasha, M. Ghadiri, A. Bayly, The effect of particle shape on predicted segregation in binary powder mixtures, Powder Technol. 319 (2017) 313–322. https://doi.org/10.1016/j.powtec.2017.06.059.
[8] G. Chen, Surface wear reduction of bulk solids handling equipment using bionic design, (2017).
[9] M.P. Fransen, M. Langelaar, D.L. Schott, Including stochastics in metamodel-based DEM model calibration, Powder Technol. 406 (2022). https://doi.org/10.1016/j.powtec.2022.117400.
[10] B. Jadidi, M. Ebrahimi, F. Ein-Mozaffari, A. Lohi, Mixing performance analysis of non-cohesive particles in a double paddle blender using DEM and experiments, Powder Technol. 397 (2022). https://doi.org/10.1016/j.powtec.2022.117122.
[11] H.P. Zhu, Z.Y. Zhou, R.Y. Yang, A.B. Yu, Discrete particle simulation of particulate systems: Theoretical developments, Chem. Eng. Sci. 62 (2007) 3378–3396. https://doi.org/10.1016/j.ces.2006.12.089.
[12] C.M. Wensrich, A. Katterfeld, Rolling friction as a technique for modelling particle shape in DEM, Powder Technol. 217 (2012) 409–417. https://doi.org/10.1016/j.powtec.2011.10.057.
[13] J. Ai, J.F. Chen, J.M. Rotter, J.Y. Ooi, Assessment of rolling resistance models in discrete element simulations, Powder Technol. 206 (2011) 269–282. https://doi.org/10.1016/j.powtec.2010.09.030.

[14] T. Roessler, C. Richter, A. Katterfeld, F. Will, Development of a standard calibration procedure for the DEM parameters of cohesionless bulk materials – part I: Solving the problem of ambiguous parameter combinations, Powder Technol. 343 (2019) 803–812. https://doi.org/10.1016/j.powtec.2018.11.034.
[15] E. Izard, M. Moreau, P. Ravier, Discrete element method simulation of segregation pattern in a sinter cooler charging chute system, Particuology. 59 (2021) 34–42. https://doi.org/10.1016/j.partic.2020.08.004.
[16] A. Chakrabarty, R. Biswas, S. Basu, S. Nag, Characterisation of binary mixtures of pellets and sinter for DEM simulations, Adv. Powder Technol. 33 (2022). https://doi.org/10.1016/j.apt.2021.11.010.
[17] A. Katterfeld, C. Coetzee, T. Donohue, J. Fottner, A. Grima, A. Ramirez Gomez, D. Ilic, R. Kačianauskas, J. Necas, D. Schott, Calibration of DEM parameters for cohesionless bulk materials under rapid flow conditions and low consolidation, White Pap. (2019).
[18] C.J. Coetzee, Review: Calibration of the discrete element method, Powder Technol. 310 (2017) 104–142. https://doi.org/10.1016/j.powtec.2017.01.015.
[19] H. Wei, H. Nie, Y. Li, H. Saxén, Z. He, Y. Yu, Measurement and simulation validation of DEM parameters of pellet, sinter and coke particles, Powder Technol. 364 (2020) 593–603. https://doi.org/10.1016/j.powtec.2020.01.044.
[20] G.K.P. Barrios, R.M. de Carvalho, A. Kwade, L.M. Tavares, Contact parameter estimation for DEM simulation of iron ore pellet handling, Powder Technol. 248 (2013) 84–93. https://doi.org/10.1016/j.powtec.2013.01.063.
[21] A. Tripathi, V. Kumar, A. Agarwal, A. Tripathi, S. Basu, A. Chakrabarty, S. Nag, Quantitative DEM simulation of pellet and sinter particles using rolling friction estimated from image analysis, Powder Technol. 380 (2021) 288–302. https://doi.org/10.1016/j.powtec.2020.11.024.
[22] C.M. Wensrich, A. Katterfeld, Rolling friction as a technique for modelling particle shape in DEM, Powder Technol. 217 (2012) 409–417. https://doi.org/10.1016/j.powtec.2011.10.057.